Large Synoptic Survey Telescope

Ellipticity Correlation of the LSST PSF and the Optimal Interpolation Scheme

M.J. Jee (UCD), J.G. Jernigan (SSL/UCB), J.R. Peterson (Purdue), J. A. Tyson (UCD), D. Burke (SLAC), S.M. Kahn (SLAC), C.F. Claver (NOAO), D. Wittman (UCD), P. Gee (UCD)

The weak lensing science goals of the Large Synoptic Survey Telescope (LSST) require that we carefully model and separate the instrumental artifacts from the intrinsic shear signal caused by gravitational lensing. The dominant source of the systematics for the LSST (and also for other ground based facilities) is the spatial correlation of the point spread function (PSF) modulated both by the atmospheric turbulence and by the optical aberration. In this work, we present our simulation of the Cerro Pachón's atmosphere with a six layer phase-screen model and its impact on the LSST's spatial PSF correlation. We also demonstrate how efficiently these systematics can be controlled with our optimal PSF interpolation scheme.

INTRODUCTION

It is paramount to understand the behavior of the point spread function (PSF) of the Large Synoptic Survey Telescope (LSST) and to correct the systematics thereof. We investigate the issue here by simulating the PSF of the telescope under the influence of both the atmospheric and the optical aberrations, and by modeling the spatial variation of the PSF across the full (3.5 degree x 3.5 degree) field-of-view with the principal component analysis (PCA) technique.

SIMULATION OF ATMOSPHERE

To simulate the effects of atmospheric turbulence, we generated 6-layer Kolmogorov phase screens with an outer scale of 20 m (Figure 1). Because the field-of-view of the LSST is large, the highest altitude layer needs to have a physical size greater than ~1 km x 1 km. In addition to this, there should be ample margins at the boundaries to allow for wind-shifts during the proposed integration of 15 secs. With the r0/pixel scale set to ~1, we choose the dimension of the phase screen to be 8192x8192, which corresponds to the physical size of 1.5 km x 1.5 km. The altitude and the weight for each layer are adopted from Ellerbroek (2002). Table 1 summarizes these values and also randomized wind velocities. Considering the highest wind velocity (~20 m/s), we chose the time step of the simulation to be 0.005 s., which corresponds to ~0.5 pixel shift for this layer (i.e., Nyquist sampling rate).

Table 1. Atmospheric Turbulence Profile

Layer	Altitude (km)	Weight	Vx (m/s)	Vy(m/s)
1	0	0.652	1.1	4.5
2	2.6	0.172	5.0	-5.1
3	5.2	0.055	8.1	5.0
4	7.7	0.025	1.9	20.1
5	12.9	0.074	10.1	15.8
6	15.5	0.022	-5.3	12.6

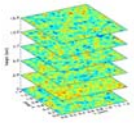

Fig. 1. Six Kolmogorov phase screens used for the simulation

SIMULATION OF OPTICAL ABERRATIONS

We randomized the Zernike coefficients for the focus (Z_4), the 0° astigmatism (Z_5), and the 45° astigmatism (Z_6) to simulate the effects of the optical aberrations. Figure 2 shows the position-dependent variation of these coefficients across the field of view. We display the ellipticity [defined as (a-b)/(a+b)] of the PSFs induced by these aberrations in Figure 3.

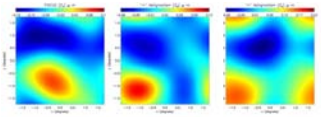

Fig. 2. Simulated optical aberrations in terms of Zernike coefficients. Combined with the focus offset Z_4, Z_6 is responsible for the elongation along x- or y- axis whereas Z_5 determines the elongation along the diagonal direction. We display the resulting variation of the PSF ellipticity in Figure 3.

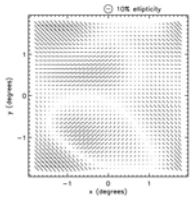

Fig. 3. "Whisker" plot showing the ellipticity of the LSST PSF due to the input aberrations illustrated in Figure 2. The sticks are aligned in the direction of the PSF elongation, and the length of the stick is proportional to the magnitude of ellipticity.

ELLIPTICITY AND SIZE VERSUS EXPOSURE TIME

In general, the ellipticity of PSF decreases as a function of exposure time. This is because, as exposure time increases, the telescope's pupil sees more uncorrelated phase screens. Here, without turning on the above optical aberrations, we purely investigated the mean PSF ellipticity and size as a function of exposure time. The decrease of mean PSF ellipticity as a function of exposure time was also observed in de Vries et al. (2007).

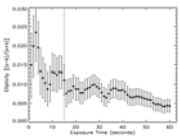

Fig 4. PSF ellipticity as a function of exposure time.

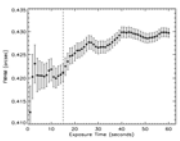

Fig 5. PSF FWHM as a function of exposure time.

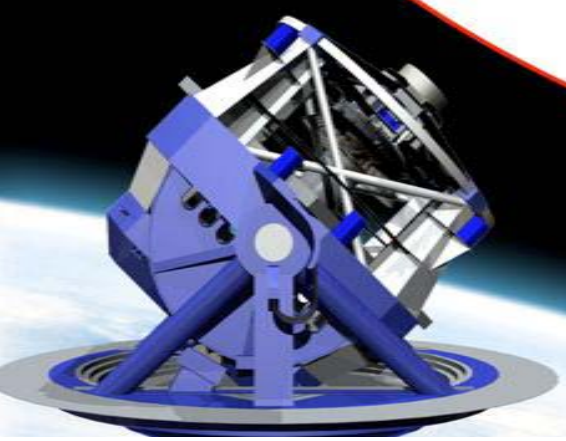

INTERPOLATION THROUGH PRINCIPAL COMPONENT ANALYSIS

In order to model the variation of PSFs, we first decompose the PSFs with some basis functions using Principal Component Analysis (PCA; Jee 2007). By construction, PCA provides the most compact basis functions for a given data set.

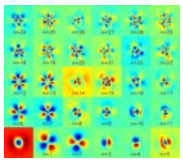

Fig. 6. The first 30 eigen-PSFs (i.e. principal components) used in the decomposition of the simulated LSST PSFs.

SIMULATION RESULTS

We randomly distributed 4000 stars in the LSST field of view and simulated their PSFs under the influence of the atmospheric and the optical aberrations. The ellipticities of the stars were measured when the exposure time reached 15 seconds. The left panel of Figure 7 shows the ellipticity distribution of these 4000 stars. We decomposed the PSFs with PCA and modeled the variation of the PC coefficients with 10th order polynomials. The middle panel of Figure 7 illustrates that our PCA interpolation closely approximates the observed (simulated) variation of the PSF ellipticity in the left panel. We display the residual ellipticity in the right panel. Another method to evaluate the fidelity of the PSF interpolation scheme is to investigate angular ellipticity correlations. We demonstrate in Figure 8 that the correlation of the residual ellipticity in a single exposure (the LSST will have hundreds of images per sky patch) is much lower than predicted cosmic shear signals.

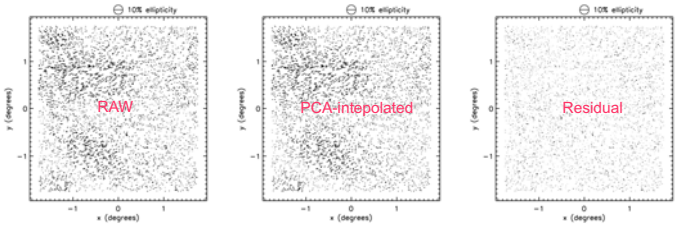

Fig. 7. Ellipticity distribution of the simulated LSST PSFs (left). The middle panel shows the ellipticity distribution of the PCA-interpolated PSFs. Comparison of these two plots along with the residual plot (right) illustrates that our PCA interpolation closely approximates the PSF variation in the LSST field.

CONCLUSIONS

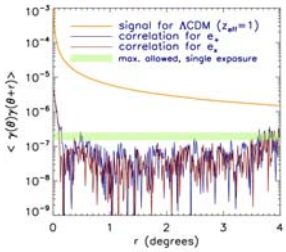

Fig. 8 Angular ellipticity correlation of the residual PSF in a single exposure.

- Longer exposure time tends to give larger and rounder PSFs. For the nominal exposure time of 15 seconds for the LSST, the typical ellipticity and the FWHM of the PSFs becomes ~0.01 and ~0.4", respectively, when only the atmospheric turbulence is included; the final seeing becomes ~0.6" because of the additional ~0.4" contribution from the detector, dome, and camera.
- When both the optical and the atmospheric aberrations are turned on, the resulting PSF anisotropy pattern resembles the feature that is already observed for the optical aberration simulation. Of course, the magnitude of the ellipticity is significantly (approximately a factor of 4) reduced because of the atmospheric circularization.
- Our PSF interpolation through PCA precisely describes the observed PSF pattern. The residual ellipticity correlation is of an order of 10^{-7}, far smaller than expected cosmic shear signals. In addition, because this PCA interpolation gives the full-blown PSF shape (not just ellipticity or FWHM), we can apply the model to objects with different sizes and radial profiles in a consistent matter.

FUTURE PLANS

- More realistic optics model of the LSST is to be added including periodic detector-focal plane errors (i.e., tiling effect), field-dependent pupil obscuration, detector charge diffusion, etc. However, the inclusion is not expected to affect residuals.
- For now, the simulation is limited to monochromatic light at 5000Å. We plan to sample the PSFs at other wavelength as well in order to generate more realistic PSFs for a given throughput curve.
- We have not observed any significant correlation between the directions of wind and PSF anisotropy such as the findings of Asztalos et al. 2007. However, this issue still needs to be explored further with different wind velocities.

REFERENCES

S. Asztalos, W. H. de Vries, L. J. Rosenberg, T. Treadway, D. Burke, C. Claver, A. Saha, and P. Puxley, 2007, ApJ, 659, 69
B. L. Ellerbroek, 2002, J. Opt. Soc. Am. 19, 1803
M. J. Jee, J. P. Blakeslee, M. Sirianni, A. R. Martel, R. L. White, and H. C. Ford, 2007, PASP, in press (arXiv:0710.5560)
W. H. de Vries, S. S. Olivier, S. J. Asztalos, L. J. Rosenberg, K. L. Baker, 2007, ApJ, 662, 744

LSST is a public private partnership. Design and development activity is supported by in part the National Science Foundation under Scientific Program Order No. 9 (AST-0551161) and Scientific Program Order No. 1 (AST-0244680) through Cooperative Agreement AST-0132798. Portions of this work are supported by the Department of Energy under contract DE-AC02-76SF00515 with the Stanford Linear Accelerator Center, contract DE-AC02-98CH10886 with Brookhaven National Laboratory, and contract W-7405-ENG-48 with Lawrence Livermore National Laboratory. Additional funding comes from private donations, grants to universities, and in-kind support at Department of Energy laboratories and other LSSTC Institutional Members.

Brookhaven National Laboratory, California Institute of Technology, Columbia University, Google Inc., Harvard-Smithsonian Center for Astrophysics, Johns Hopkins University, Kavli Institute for Particle Astrophysics and Cosmology - Stanford University, Las Cumbres Observatory Inc., Lawrence Livermore National Laboratory, National Optical Astronomy Observatory, Princeton University, Purdue University, Research Corporation, Stanford Linear Accelerator Center, The Pennsylvania State University, The University of Arizona, University of California at Davis, University of California at Irvine, University of Illinois at Urbana-Champaign, University of Pennsylvania, University of Pittsburgh, University of Washington